# Estimation of Dynamic, In Vivo Soft-Tissue Deformation: Experimental Technique and Application in a Canine Model of Tendon Injury and Repair

Michael J. Bey,[1] Stephanie K. Kline,[1] Andrew R. Baker,[2] Jesse A. McCarron,[3] Joseph P. Iannotti,[3] Kathleen A. Derwin[2]

[1]Bone and Joint Center, Henry Ford Hospital, 2799 W. Grand Boulevard, Detroit, Michigan 48202, [2]Department of Biomedical Engineering, Cleveland Clinic, ND-20, 9500 Euclid Avenue, Cleveland, Ohio 44195, [3]Department of Orthopaedics, Cleveland Clinic, 9500 Euclid Avenue, Cleveland, Ohio 44195

*Received 8 April 2010; accepted 8 October 2010*
*Published online in Wiley Online Library (wileyonlinelibrary.com). DOI 10.1002/jor.21315*

**ABSTRACT:** Outcomes after rotator cuff surgery are typically assessed with measures of strength, joint motion, or pain, but these measures do not provide a direct assessment of tissue function as healing progresses. To address this limitation, this manuscript describes biplane X-ray analysis as a technique for quantifying in vivo soft-tissue deformation. Tantalum beads were implanted in the humerus and infraspinatus tendon in a canine model of tendon injury and repair. Biplane X-ray images were acquired during treadmill trotting and tissue deformation was estimated from the three-dimensional bead positions. Changes over time were characterized by the mean, range, and normalized range (i.e., range/mean) of interbead distance. Intact tendon repair tissue demonstrated significant decreases over time in the mean ($p = 0.003$), range ($p = 0.001$), and normalized range ($p = 0.001$) of interbead distance. Failed tendon repair tissue demonstrated significant decreases over time in the range ($p = 0.05$) and normalized range ($p = 0.04$) of interbead distance. In an uninjured control, differences over time in the interbead distance parameters were not detected. This approach is a promising technique for estimating changes over time in soft-tissue deformation. These preliminary data indicate appreciable differences between normal tendons, intact repairs, and failed repairs. © 2010 Orthopaedic Research Society Published by Wiley Periodicals, Inc. J Orthop Res

**Keywords:** tendon; in vivo; biplane X-ray; animal model; imaging

Tendon injuries are very common and have a major impact on the cost of medical care and days lost from productive occupations. For example, rotator cuff injuries affect approximately 30–40% of the population over age 60.[1–3] Surgical repair of chronic tears is indicated when conservative treatment fails to improve the patients' symptoms.[4] Despite improvements in the understanding of rotator cuff pathology and advances in surgical options, repairs of large rotator cuff tears fail in 20–95% of cases.[5–7] The outcome of rotator cuff repair surgery is typically assessed by measuring muscle strength, joint range of motion, pain, and other subjective indicators of function. Although these outcomes are used routinely, they do not offer a direct means of evaluating the functional quality (e.g., stiffness or modulus) of the repair tissue as healing progresses. Thus, the treating physician must make a best judgment as to the timing and nature of post-operative activity without knowing the mechanical capabilities of the healing tissues, which may in turn contribute to the higher rates of post-operative repair failure.

Various techniques are available for assessing the quality of tendon repair tissues under in vivo conditions. Direct approaches measure forces or strains with devices such as strain gauges,[8,9] buckle transducers,[10,11] and implantable force transducers.[12–15] Although these instruments have provided valuable information regarding in vivo tissue properties, buckle transducers and implantable force transducers are affected by many factors (e.g., sensor orientation) and the highly invasive nature of surgical implantation makes follow-up studies impractical. More recently, radiostereometric analysis (RSA) has been used to investigate deformation in ligament grafts[16,17] and healing tendons[18,19] over time. RSA determines the three-dimensional (3D) position of implanted radio-opaque markers from a pair of static radiographic images, and is useful for assessing graft stretching, fixation slippage, or gap formation across a soft-tissue repair. However, estimates of tissue deformation during dynamic activities are necessary to assess dynamic function of a healing tendon, and these data cannot be obtained with RSA. Thus, while these techniques have contributed significantly to our general understanding of joint and soft-tissue injuries, none are suited to assess the functional properties of the repair tissue itself. Without appropriate tools for directly assessing the quality of healing tendon repairs in vivo, it is difficult to objectively assess and optimize the treatment of tendon injuries.

We have adapted the use of biplane X-ray analysis for studying dynamic, in vivo tendon deformation. Biplane X-ray analysis was developed for measuring 3D in vivo joint motion by tracking the position of tantalum beads implanted in bone during dynamic activities to within $\pm 0.1$ mm.[20] This approach has been used to study motion of the canine knee[20,21] and human knee.[22,23] We have adapted this technique to directly monitor healing tendons in vivo by tracking the 3D position of tantalum beads sutured to the surface of the healing infraspinatus tendon in the canine shoulder. The objective of this manuscript is to describe the use of biplane X-ray analysis to estimate dynamic, in vivo soft-tissue deformation and to demonstrate application of this technique using a canine model of tendon injury and repair.

Correspondence to: Michael J. Bey (T: +1-313-916-8683; F: +1-313-916-8812. E-mail: bey@bjc.hfh.edu)

© 2010 Orthopaedic Research Society. Published by Wiley Periodicals, Inc.

## METHODS

### Overview

The experimental approach for estimating dynamic, in vivo tendon deformation consisted of: (1) implanting tantalum beads into the humerus and onto the infraspinatus tendon in a canine model of rotator cuff tendon injury and repair, (2) acquiring high-speed radiographic images during treadmill activity with a biplane X-ray system, (3) determining the 3D tantalum bead positions from the biplane X-ray images, and (4) calculating joint kinematics and estimating repair tissue deformation throughout the healing process by measuring changes in the 3D interbead (i.e., bead-to-bead) distance. These steps are described in additional detail here.

### Animal Model of Tendon Injury and Repair

The canine rotator cuff model used for this feasibility study involved release and repair of a portion of the infraspinatus tendon.[24] Three adult mongrel dogs (2–4 years, 25–35 kg) were used. All procedures were approved by the Institutional Animal Care and Use Committee at the Cleveland Clinic.

Dogs were initially anesthetized with an intravenous dose of sodium pentothal (20 mg/kg) to effect and then intubated and maintained on isoflurane in oxygen (3%). The infraspinatus tendon was approached using a transverse incision from the lateral aspect of the acromion to the greater tuberosity. In two dogs, the superior two-thirds of the infraspinatus tendon was detached from the humerus and the adjacent, intact inferior one-third of the infraspinatus tendon (Fig. 1A). A large (15 mm $\times$ 20 mm) portion of joint capsule was excised starting at the glenoid rim and extending laterally (Fig. 1A). The bone at the tendon insertion site was lightly decorticated. No injury was created in the third dog, which served as a normal control.

In the two dogs undergoing tendon injury and repair, the infraspinatus tendon was repaired back to its insertion on the humerus via two trans-osseous, modified Mason-Allen sutures (Arthrex, Inc., Naples, FL) using 0-FiberWire$^{TM}$ (Fig. 1B). One 1.6 mm tantalum bead (Tilly Medical Products, Lund, Sweden) with a laser-drilled 0.5 mm hole was sewn onto the surface of the released portion of the infraspinatus tendon approximately 20 mm from the repair site (Fig. 1B). A second tantalum bead was impacted approximately 1 mm into the humeral head at the infraspinatus insertion site, immediately lateral to the repair and in line with the direction of pull of the infraspinatus tendon (Fig. 1B). These bead locations were selected based on the goal of spanning the repair site from the lateral edge of the tendon attachment to the medial edge of the repair sutures. Beads were implanted in the same locations in the control dog. In two of the dogs, two additional beads were implanted into the humeral diaphysis and three beads were implanted into the scapula in order to measure joint kinematics (specifically, flexion/extension, abduction/adduction, and internal/external rotation).[20]

Post-operatively, all dogs were allowed full weight bearing, but housed in low-ceiling runs to reduce their activity. Standard X-rays were obtained at surgery and 2 weeks post-surgery to make a gross determination of whether or not the tendon repair was intact (Fig. 1C). This was accomplished by assessing the position of the tendon bead relative to the humerus. At 2 weeks post-surgery, we determined that one experimental dog had an intact repair (interbead distance changed less than 3.5 mm) and one dog had a failed tendon repair (interbead distance changed 9 mm and was subsequently observed to move independently from the bone during dynamic activity at early time points). The interbead distance in the control dog was unchanged from the time of surgery. Thus, the three dogs used in this feasibility study represented: (1) an intact tendon repair, (2) a failed tendon repair, and (3) a normal control dog with no tendon injury or repair.

### Biplane X-ray Image Acquisition

Following treadmill training, dynamic biplane X-ray images were collected during treadmill trotting at 2- to 4-week intervals starting at 2 weeks post-surgery. The images were collected at 100 Hz during slow trotting (i.e., the speed at which each dog broke into a trot), and three trials were collected at each time point. The treadmill speed determined during the first testing session was used for all sessions.

### Estimation of Repair Tissue Deformation

Custom software was used to determine the 3D position of each implanted tantalum bead to within $\pm$0.1 mm.[20] Repair tissue deformation was estimated by calculating the 3D distance between the bead implanted in the humerus and the bead affixed to the infraspinatus tendon during dynamic activity. To insure that our estimated measures of repair tissue deformation included only the portion of the gait cycle where the infraspinatus tendon is considered to be under load, we restricted the bead analyses to the portion of the gait cycle from paw-strike to mid-stance of each trial. This portion of the gait cycle was chosen based on previous research which has shown through electromyography (EMG) analysis that the infraspinatus muscle is active during trotting from the "aft-swing" through the "mid-stance" phases of the gait cycle.[25] Paw-strike, paw-off, and mid-stance phases of the gait cycle were estimated by direct observation of the biplane X-ray images.

### Estimating Changes In Repair Tissue Deformation Over Time

Repair tissue deformation was estimated at 2, 5, 8, 13, 17, 20, and 28 weeks of healing. Tissue deformation was described by the range and the baseline position (i.e., mean) of 3D interbead

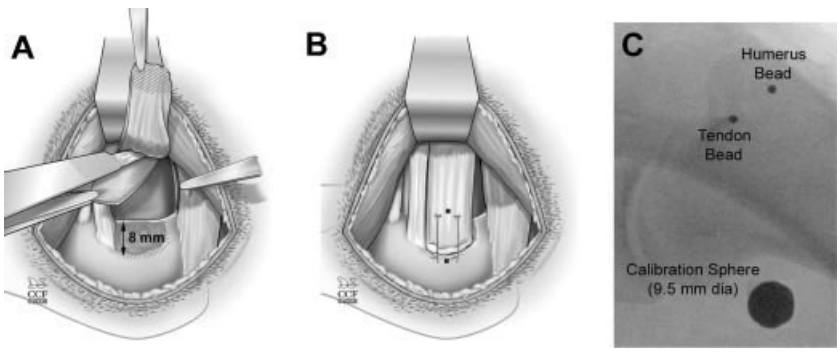


**Figure 1.** The canine injury model: (A) A superior two-thirds injury of the infraspinatus tendon was created and a portion of underlying joint capsule was resected. (B) The tendon was repaired to bone using two transosseous sutures. Tantalum beads (shown as black dots ●) were sewn onto the surface of the infraspinatus tendon and implanted into the humerus at the repair site. (C) Intra-operative X-ray shows the tendon bead, bone bead, and calibration sphere (large circle).

distance. In addition to the range and mean of interbead distance, we normalized the range by the mean to obtain a parameter that is independent of the initial distance between the tantalum beads (which can not be precisely controlled from dog to dog). This normalized range of interbead distance can be used to make comparisons between individual dogs at any time point. Thus our analyses used mean, range, and normalized range (range divided by mean) of interbead distance to estimate tissue deformation from paw-strike to the mid-stance of gait for each dog over the healing period.

### Statistical Analysis

To assess the extent to which the mean, range, and normalized range of interbead distance changed over time, data from the three trials at each time point were averaged and regression analysis was used to assess a dependence on time. Similarly, regression analysis was also used to assess the extent to which the maximum and minimum joint angles (i.e., flexion/extension, abduction/adduction, and internal/external rotation) determined from the kinematic analysis in two dogs changed over time. Significance was set at $\alpha = 0.05$.

## RESULTS

The 3D distance between the implanted tantalum beads on the infraspinatus tendon and the proximal humerus oscillated throughout each gait cycle (Fig. 2). These changes in interbead distance were in response to changes in joint motion (i.e., passive tendon stretch) and changes in muscle loading (i.e., active tendon stretch). Note that the paw-strike, paw-off, and mid-stance phases of the gait cycle corresponded with inflection points of the flexion/extension angle of the shoulder (Fig. 2). As previously explained, to confidently estimate deformation of the infraspinatus tendon repair tissue, we restricted our analyses of interbead distances to the portion of the gait cycle from paw-strike to mid-stance of each trial where the repaired tendon is believed to be under load based on prior EMG studies.[25]

The dog with the intact tendon repair demonstrated marked changes in interbead distance over 28 weeks of healing (Fig. 3). Mean interbead distance decreased significantly with time ($p = 0.003$), suggesting that the tendon repair contracted approximately 19% over 28 weeks (Fig. 4). The range of interbead distance decreased significantly with time ($p = 0.001$), suggesting that the healing tendon repair became 70% stiffer over 28 weeks (Fig. 5).

In the failed repair, the mean interbead distance did not depend on time ($p = 0.96$, Fig. 4), suggesting that limited contracture occurs in any new scar tissue that may form across a ruptured tendon repair, at least over this time period. However, the range of interbead distance did significantly decrease over time ($p = 0.05$, Fig. 5), suggesting a stiffening (or maturation) of scar tissue may be occurring between 13 and 17 weeks.

In the control dog, the mean interbead distance tended to increase slightly over time but this increase was not statistically significant ($p = 0.06$, Fig. 4). We propose that this increase of approximately 0.5 mm would be insignificant from a clinical perspective. The range of interbead distance did not depend on time in the control dog ($p = 0.49$, Fig. 5).

The normalized range of interbead distance significantly decreased over time in the intact ($p = 0.001$) and failed ($p = 0.04$) tendon repairs, reaching control levels only in the intact tendon repair by 17 weeks (Fig. 6). The normalized range of interbead distance in the control dog was not dependent on time ($p = 0.45$) and averaged $4.2 \pm 1.5\%$ across all five time points.

For the two dogs in which kinematic analyses were performed, differences over time were not detected in the maximum or minimum values for flexion/extension angle ($p > 0.13$), abduction/adduction angle ($p > 0.19$), or internal/external rotation angle ($p > 0.19$). These data suggest that these dogs were performing the treadmill activity in the same manner over time.

## DISCUSSION

The objective of this manuscript was to describe the use of biplane X-ray analysis to estimate dynamic, in vivo

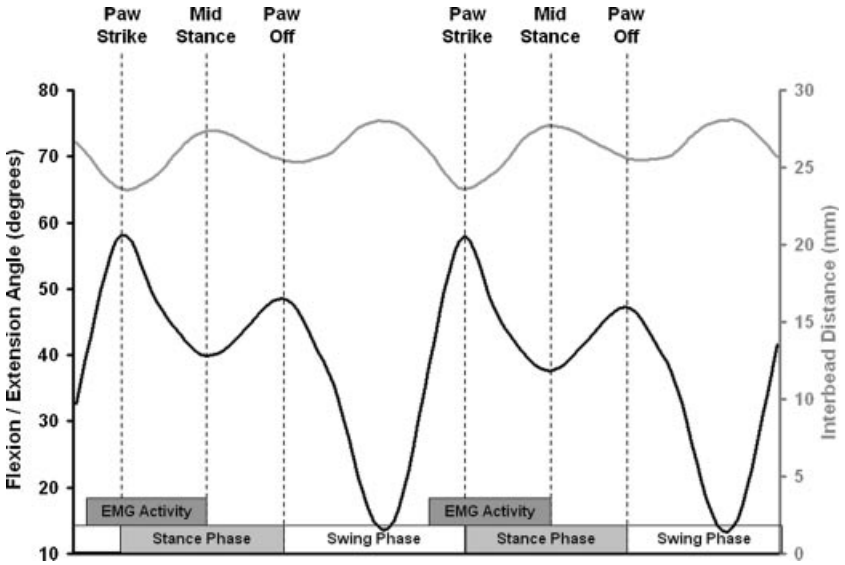


**Figure 2.** Flexion/extension angle (left axis) and 3D interbead distance (right axis) demonstrated an inverse relationship, with the local maxima/minima of flexion/extension corresponding to the local minima/maxima of interbead distance. "EMG Activity" indicates the portion of the gait cycle where the infraspinatus is under load according to previous research by Tokuriki.[25]

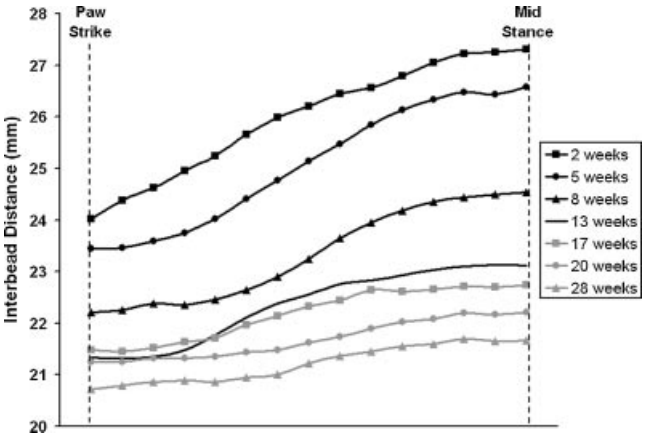


**Figure 3.** Interbead distance from a dog with an intact tendon repair. Curves are the average of three trials of interbead distance measured during slow trot activity from 2 to 28 weeks post-surgery. Decreases in the range and mean interbead distance over this time period are readily apparent and suggest changes in the healing tendon's structural properties.

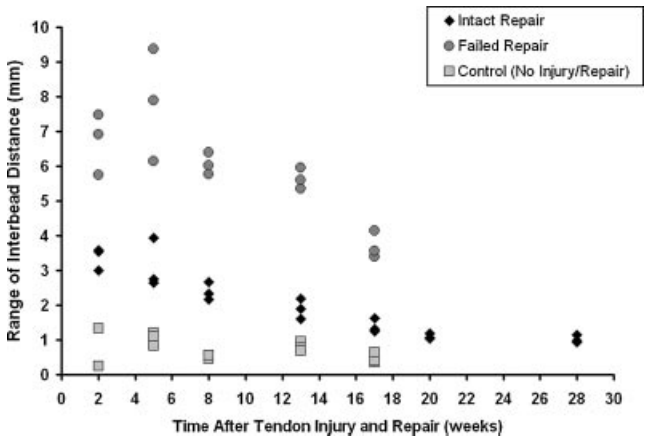


**Figure 5.** Range of interbead distance in an intact repair (◆), a failed repair (●), and a control dog (■). Data from three trials at each time point are shown. The range of interbead distance decreased over time in the intact ($p = 0.001$) and failed ($p = 0.05$) repairs.

soft-tissue deformation and to demonstrate application of this technique using a canine model of tendon injury and repair. The study demonstrated that biplane X-ray analysis is a sensitive tool for quantifying changes in in vivo repair tissue deformation and joint kinematics following injury and repair in the canine model. In particular, the 1–5 mm change over time in interbead distance parameters (measured during only the portion of the gait cycle where the infraspinatus tendon is considered to be under load) is at least an order of magnitude greater than the accuracy of the measurement technique.

We estimated repair tissue deformation by both the range and the baseline position (i.e., mean) of interbead distance during dynamic activity. Since we extracted the data from the portion of the gait cycle where the muscle is firing, we believe that bead oscillations reflect tissue deformation across the repair site. In the case of the failed repair, our previous research has demonstrated that "robust scar tissue forms in the gap between the failed tendon end and the humerus, which can be visually, mechanically, and histologically misconstrued as tendon."[26] Scar tissue too is expected to remodel over time, and it is likely in the case of failed repair that we are quantifying these changes. A decrease in the range of interbead distance for a given activity suggests that tissue compliance is decreasing over time (i.e., the tissue is getting stiffer). A decrease in the baseline (or mean) of interbead distance suggests that tissue contracture may be occurring over time (i.e., the overall distance between the tendon and humerus beads is decreasing independent of shoulder motion or muscle activity).

This feasibility study demonstrated statistically and clinically significant decreases in the mean, range, and normalized range of interbead distance over time in intact tendon repair. The data also demonstrated that these parameters are markedly different between normal tendons, intact repairs, and failed repairs. For the

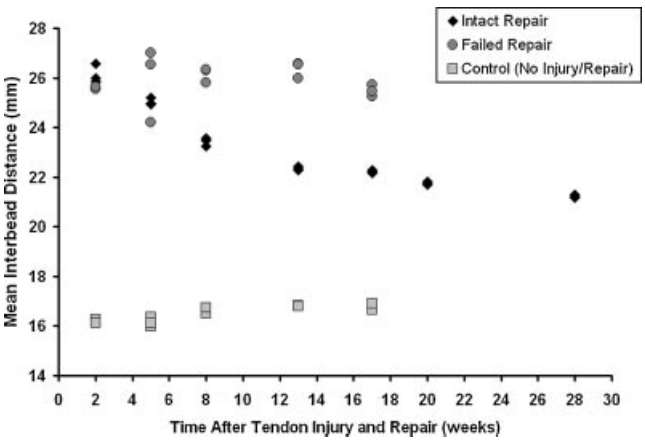


**Figure 4.** Mean interbead distance in an intact repair (◆), a failed repair (●), and a control dog (■). Data from three trials at each time point are shown. Mean interbead distance decreased over time in the intact repair ($p = 0.003$).

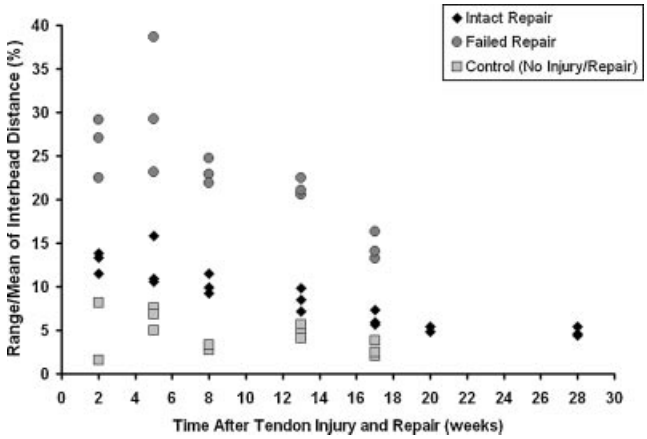


**Figure 6.** Normalized range of interbead distance in an intact repair (◆), a failed repair (●), and a control dog (■). Data from three trials at each time point are shown. Normalized range of interbead distance decreased over time in the intact ($p = 0.001$) and failed ($p = 0.04$) repairs.

intact repair, changes in mean interbead distance may reflect repair contracture of approximately 19%, while changes in the range of interbead distance may reflect an increase in repair stiffness of approximately 70% over 28 weeks of healing. The normalized range of interbead distance in intact tendon repair appears to approach normal levels (approximately 5%) by 17 weeks after repair. In failed repairs, the mean interbead distance did not change over time, suggesting that limited contracture occurs in any new scar tissue that may form across a ruptured tendon repair, at least during the first 17 weeks after surgery. However, the range of interbead distance did significantly decrease over time, suggesting a stiffening (or maturation) of scar tissue may be occurring by 17 weeks. As expected, interbead distances did not change over time in normal tendons.

The findings from this feasibility study are corroborated by a recent study in human subjects, where tantalum beads were implanted in Achilles tendon on either side of the surgical repair site.[19] At 6, 12, 18, and 52 weeks after surgery, the healing tendons were subjected to two static load conditions and RSA was performed. Because interbead distance was measured at two static loads, the mechanical properties of the healing repair tissue could be estimated. The stiffness and modulus of the healing tendons increased over time, which parallels our findings of a decreased range of interbead distance in healing tendon over time. While this previous study did not estimate repair tissue deformation during true dynamic activity, it does demonstrate the potential for using 3D tissue deformations to estimate the mechanical properties of healing soft tissues.

The use of biplane X-ray analysis to estimate dynamic, in vivo soft-tissue deformations is not without limitation. First, the muscle forces acting on the repair during activity are not known, so absolute tissue stiffness cannot be computed and interpretation of tissue deformation parameters must be made by comparison to the first postoperative time point. This limitation requires the subject perform the activity in the same way over time. Analysis of the joint kinematic data in two dogs indicated that the manner in which each dog performed the treadmill trotting activity did not change over time. Thus, we conclude that the time-dependent changes in interbead distance that were measured over time in these same dogs were not a consequence of a systematic change in the manner in which the dogs performed the treadmill trotting. In the future, it may be possible to use an instrumented treadmill to estimate the forces in the shoulder tendons and/or implantable transducers to directly monitor force in the infraspinatus tendon during dynamic activity. Another concern with this method is the possibility of bead migration over time, which has been shown previously with beads implanted within soft tissue grafts.[16,17] In our study we sutured the beads to the tendons and showed that the outcome measures did not change over time for the normal tendon. This result supports the conclusion that the beads do not migrate in any appreciable way over time for this attachment method. Lastly, this feasibility study used only one pair of beads, which were placed in such a way as to span the tendon repair site. While a multi-bead array may have provided additional information about nonuniform soft tissue deformation across the tendon width, the canine infraspinatus tendon is highly aligned, independent from the other rotator cuff tendons, and is likely loaded in uniaxial tension. Thus, the repair tissue deformation is expected to be primarily one-dimensional and for the purposes of this feasibility study could be estimated by a single bead placed in the tendon.

In summary, we have adapted a biplane X-ray system (originally developed for measuring in vivo joint motion) to estimate in vivo tissue deformation across the repair site of healing tendons. No other research tool currently exists that is capable of measuring 3D, in vivo joint and tissue motion during functional, dynamic activities at an accuracy of within $\pm 0.1$ mm. Future efforts will investigate the extent to which estimates of in vivo tissue deformation can be used as a surrogate measure of healing tendon quality. Specifically, using our canine model we will investigate a predictive relationship between the in vivo deformation of repaired tendons and conventional, in vitro endpoint measures of tendon biomechanics, structure, and composition. As the scientific basis of this work is established, bi-planar radiography may be an effective research tool for evaluating surgical, rehabilitation, and tissue-engineered protocols for treating tendon tears, and for studying the underlying mechanisms associated with in vivo tendon function and tendon healing.

## ACKNOWLEDGMENTS

Financial support was provided by the Henry Ford Hospital Department of Orthopaedic Surgery, NIH R21 AR052765, and NIH T32 AR050959. None of the authors have any professional or financial affiliations that may be perceived to have biased the presentation of this information.

## REFERENCES

1. Milgrom C, Schaffler M, Gilbert S, et al. 1995. Rotator-cuff changes in asymptomatic adults. The effect of age, hand dominance and gender. J Bone Joint Surg Br 77:296–298.
2. Tempelhof S, Rupp S, Seil R. 1999. Age-related prevalence of rotator cuff tears in asymptomatic shoulders. J Shoulder Elbow Surg 8:296–299.
3. Yamaguchi K, Tetro AM, Blam O, et al. 2001. Natural history of asymptomatic rotator cuff tears: a longitudinal analysis of asymptomatic tears detected sonographically. J Shoulder Elbow Surg 10:199–203.
4. Mantone JK, Burkhead WZ Jr, Noonan J Jr. 2000. Nonoperative treatment of rotator cuff tears. Orthop Clin North Am 31:295–311.
5. Galatz LM, Ball CM, Teefey SA, et al. 2004. The outcome and repair integrity of completely arthroscopically repaired large and massive rotator cuff tears. J Bone Joint Surg Am 86:219–224.
6. Gazielly DF, Gleyze P, Montagnon C. 1994. Functional and anatomical results after rotator cuff repair. Clin Orthop Relat Res 304:43–53.

7. Harryman DT II, Mack LA, Wang KY, et al. 1991. Repairs of the rotator cuff. Correlation of functional results with integrity of the cuff. J Bone Joint Surg Am 73:982–989.
8. Brown TD, Sigal L, Njus GO, et al. 1986. Dynamic performance characteristics of the liquid metal strain gage. J Biomech 19:165–173.
9. Riemersma DJ, van den Bogert AJ, Jansen MO, et al. 1996. Tendon strain in the forelimbs as a function of gait and ground characteristics and in vitro limb loading in ponies. Equine Vet J 28:133–138.
10. An KN, Berglund L, Cooney WP, et al. 1990. Direct in vivo tendon force measurement system. J Biomech 23:1269–1271.
11. Komi PV. 1990. Relevance of in vivo force measurements to human biomechanics. J Biomech 23:23–34.
12. Finni T, Komi PV, Lukkariniemi J. 1998. Achilles tendon loading during walking: application of a novel optic fiber technique. Eur J Appl Physiol Occup Physiol 77:289–291.
13. Fleming BC, Good L, Peura GD, et al. 1999. Calibration and application of an intra-articular force transducer for the measurement of patellar tendon graft forces: an in situ evaluation. J Biomech Eng 121:393–398.
14. Korvick DL, Cummings JF, Grood ES, et al. 1996. Use of an implantable force transducer to measure patellar tendon forces in goats. J Biomech 29:557–561.
15. Platt D, Wilson AM, Timbs A, et al. 1994. Novel force transducer for the measurement of tendon force in vivo. J Biomech 27:1489–1493.
16. Roos PJ, Hull ML, Howell SM. 2004. How cyclic loading affects the migration of radio-opaque markers attached to tendon grafts using a new method: a study using roentgen stereophotogrammetric analysis (RSA). J Biomech Eng 126:62–69.
17. Smith CK, Hull ML, Howell SM. 2005. Migration of radio-opaque markers injected into tendon grafts: a study using roentgen stereophotogrammetric analysis (RSA). J Biomech Eng 127:887–890.
18. Cashman PM, Baring T, Reilly P, et al. 2010. Measurement of migration of soft tissue by modified Roentgen stereophotogrammetric analysis (RSA): validation of a new technique to monitor rotator cuff tears. J Med Eng Technol. 34:159–165.
19. Schepull T, Kvist J, Andersson C, et al. 2007. Mechanical properties during healing of Achilles tendon ruptures to predict final outcome: a pilot Roentgen stereophotogrammetric analysis in 10 patients. BMC Musculoskelet Disord 8:116.
20. Tashman S, Anderst W. 2003. In-vivo measurement of dynamic joint motion using high speed biplane radiography and CT: application to canine ACL deficiency. J Biomech Eng 125:238–245.
21. Anderst WJ, Les C, Tashman S. 2005. In vivo serial joint space measurements during dynamic loading in a canine model of osteoarthritis. Osteoarthr Cartil 13:808–816.
22. Tashman S, Collon D, Anderson K, et al. 2004. Abnormal rotational knee motion during running after ACL reconstruction. Am J Sports Med 32:975–983.
23. Anderst WJ, Tashman S. 2003. A method to estimate in vivo dynamic articular surface interaction. J Biomech 36:1291–1299.
24. Derwin KA, Codsi MJ, Milks RA, et al. 2009. Rotator cuff repair augmentation in a canine model with use of a woven poly-L-lactide device. J Bone Joint Surg Am 91:1159–1171.
25. Tokuriki M. 1973. Electromyographic and joint-mechanical studies in quadrupedal locomotion. II. Trot. Nippon Juigaku Zasshi 35:525–533.
26. Derwin KA, Baker AR, Codsi MJ, et al. 2007. Assessment of the canine model of rotator cuff injury and repair. J Shoulder Elbow Surg 16:S140–S148.